Melting Mechanisms at the Limit of Superheating

Z. H. Jin,[1,2,*] P. Gumbsch,[2] K. Lu,[1] and E. Ma[3]

[1]*State Key Lab of RSA, Institute of Metal Research, Chinese Academy of Sciences, Shenyang 110015, China*
[2]*Max-Planck-Institut für Metallforschung, 70174 Stuttgart, Germany*
[3]*Department of Materials Science and Engineering, The Johns Hopkins University, Baltimore, Maryland 21218*

(Received 30 August 2000; published 12 July 2001)

The atomic-scale details during melting of a surface-free Lennard-Jones crystal were monitored using molecular dynamics simulations. Melting occurs when the superheated crystal spontaneously generates a sufficiently large number of spatially correlated destabilized particles that simultaneously satisfy the Lindemann and Born instability criteria. The accumulation and coalescence of these internal local lattice instabilities constitute the primary mechanism for homogeneous melt nucleation inside the crystal, in lieu of surface nucleation for equilibrium melting. The vibrational and elastic lattice instability criteria as well as the homogeneous nucleation theory all coincide in determining the superheating limit.

DOI: 10.1103/PhysRevLett.87.055703 PACS numbers: 64.70.Dv, 64.60.Qb

Unlike supercooling of liquids, superheating of crystalline solids is difficult due to melt nucleation at surfaces [1,2]. However, by suppressing surface melting [3,4], superheating to temperatures well above the equilibrium melting points has been achieved. It is of fundamental interest to understand the two different modes of melting, one initiated at surfaces, and the other inside the bulk interior undergoing superheating [5]. The upper limit for the superheating of a surface-free perfect crystal, as proposed by a number of authors over the past decade [6–10], is set by a succession of instability points for the crystalline state. This hierarchy of stability limits includes the isochoric (i.e., a temperature at which the liquid and the superheated solid have the same volume [6]), the isenthalpic (equal enthalpy) [7], and eventually the isentropic (equal entropy) conditions [7]. However, these outer bounds will be preempted by a rigidity catastrophe due to vanishing shear modulus [6,8], known as the Born elastic shear instability criterion [9]. Recently, a second inner bound based on a kinetic stability was added, by viewing melting as a process of thermally activated nucleation of the liquid phase inside a superheated crystal [10]. The temperature at which spontaneous, massive homogeneous nucleation occurs was suggested as a superheating limit preempting all the catastrophes listed above.

This Letter addresses the interrelationship among these melting mechanisms with the question whether the two inner bounds of the superheating limits coincide with each other. A direct link is established between these models and the Lindemann criterion well known for normal thermodynamic melting at the equilibrium melting temperature, which stipulates that melting is a vibrational lattice instability initiated at surfaces when the root-mean-square displacement (rmsd) of the atoms reaches a critical fraction of the interatomic distance [2,11,12].

Molecular dynamics (MD) simulation was used because it allows substantial metastable superheating of perfect crystals without suffering from surface/interfaces as heterogeneous nucleation sites for melting [13]. MD further allows tracking the physical properties of the atoms not only as global averages but also locally. This capability is indispensable for the exploration of a correlation between the theories and the atomic-level mechanisms at the onset of melting.

A model of 6912 Lennard-Jones (LJ) particles in a fcc cubic box with 3D periodic boundary conditions was used to represent an initially surface-free and defect-free ideal crystal. The interaction energy between two particles is given by $\phi_{\mathrm{LJ}} = r^{-12} - 2r^{-6}$, with the well depth, ε, as the unit of energy and interatomic distance, r, measured in units of $r_0 = 2^{1/6}\sigma$, where σ is the LJ diameter. All quantities are reported in reduced units: length in units of σ, temperature T in units of ε/k_B, time in units of $\tau = (\sigma^2 m/\varepsilon)^{1/2}$, where m is the mass of an LJ particle, and pressure in units of $100\varepsilon/\sigma^3$. MD is performed by rescaling velocities of the particles using the explicit Verlet algorithm [14] with a time step of 0.02τ under the zero pressure condition. Heating is done in a step-by-step procedure. After 2500 MD time steps at a temperature T, the zero pressure condition is readjusted and T is increased by ΔT for the next 2500 steps. The smallest ΔT used is 0.42×10^{-3}, equivalent to a heating rate of about 50 K/ns for argon ($\sigma = 3.405$ Å, $\varepsilon = 119.8\ k_B$).

The first-order melting transition manifests itself at $T_m = 0.79$ where the mean atomic volume (Ω) undergoes a sudden upward jump, as marked in Fig. 1(a). The melting temperature is almost 20% above the equilibrium melting point ($T_E = 0.66$ [15]). Note that even after long runs (up to 1×10^6 time steps) at $T = 0.775$ ($\Omega = 1.11$), no signal for melting can be detected, indicating the existence of a substantial metastable superheating. Unstable superheating due to the melting kinetics during the rapid heating is insignificant because of the transient nature of melting at such a high degree of superheating [16].

First, the applicability of the Born shear instability criterion was checked by calculating the elastic constants of the crystal, in particular, the shear moduli $C' = (C_{11}\text{-}C_{12})/2$ and C_{44} [17]. The stability limit of a "Born crystal" can

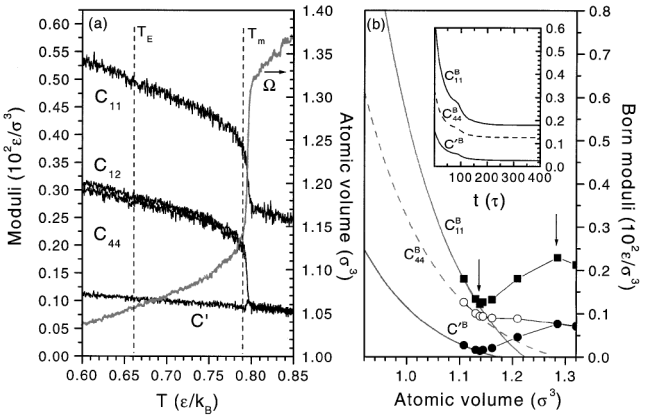

FIG. 1. (a) The T dependence of the atomic volume (Ω) and elastic moduli for the LJ crystal. Dashed lines denote the equilibrium melting point and the superheating limit, respectively. (b) The Born elastic moduli versus atomic volume. Symbols were determined for snapshot configurations after LEM (inset for a snapshot recorded at $T = 0.76$); the lines are calculated for an ideal fcc solid via pure dilation of the lattice at 0 K. Arrows denote the volumes at the onset and the end of melting.

be identified by monitoring the volume dependence of the shear moduli through a homogeneous dilation of a cubic lattice at 0 K [lines in Fig. 1(b)]. Consistent with earlier experimental and theoretical work [6,8,13], C' vanishes at a volume of 1.16 (the volume of the liquid at T_E), slightly above 1.14 at which melting starts for a superheated crystal [Fig. 1(a)]. The results confirm again that the Born criterion is not a condition for equilibrium melting but a relevant triggering mechanism for homogenous ("mechanical") melting [8,13].

In the simulated crystal, the T-dependent elastic constants were calculated as [8,18–20]

$$C_{ijkl}(T) = \langle C^B_{ijkl}\rangle + \langle C^P_{ijkl}\rangle + \langle C^K_{ijkl}\rangle, \qquad (1)$$

where the first, second, and third terms on the right-hand side of Eq. (1) represent the Born (static), the microscopic stress tensor (pressure), and the kinetic energy (thermal) contributions, respectively. The bracket represents the ensemble average during the time interval when T and system volume are kept constant. The results have also been included in Fig. 1(a). C' decreases almost linearly with increasing T but does *not* vanish at melting. Because the second term in Eq. (1) is always negative and the third term is very small [e.g., at $T = 0.76$, $C_{11} = 0.42$ $(0.65; -0.26; 0.03)$; $C_{12} = 0.23$ $(0.33; -0.10; 0)$; $C_{44} = 0.22$ $(0.33; -0.12; 0.01)$, where the three terms in Eq. (1) are given in the parentheses, the nonvanishing shear moduli must be due to the Born term when a high concentration of displaced atoms including incipient or metastable Frenkel pairs is present through fluctuations in a hot crystal (for metals with much larger Born moduli this contribution would be relatively small). Their influence was assessed by calculating the local Born moduli around a relaxed point defect. The positive contribution from an interstitial is found always larger than the negative contribution from a vacancy. We also examined how the Born moduli would change when the defects and the positional fluctuations are eliminated. This was done by recording several snapshots at a selected T and performing a local-energy minimization (LEM) with each of them [21]. The elastic constants first decreased continuously and then reached steady values [e.g., inset in Fig. 1(b)]. The moduli obtained after LEM [symbols in Fig. 1(b)] indeed coincide with those from pure dilation at 0 K.

In Fig. 1(a), at T_m the MD system deviates slightly from the Cauchy relation C_{12}-$C_{44} = 0$, which however is strictly satisfied by the Born term [Fig. 1(b)] (see Baskes [15]). After melting started, we continued to calculate "elastic constants" only to observe the isotropic property expected eventually for the liquid. The "moduli" calculated as such would be all related to the bulk modulus B, $C_{11} = 3C_{12} = 3C_{44} = 3C' = 5B/9$, where $B = (C_{11} + 2C_{12})/3$. Indeed, Fig. 1(b) shows that C^B_{11} increased significantly during melting, while C^B_{12} or C^B_{44} decreased slightly. As a result, C'^B rose gradually and finally became equal to C^B_{44}. The isotropic condition of vanishing shear moduli difference $\Delta C_S = C_{44}$-$C' = 0$ is also satisfied when all the terms in Eq. (1) are included [Fig. 1(a)]. This condition therefore marks the end of the melting transition, and was also found applicable to heterogeneous melting at a surface or interface near T_E [22]. These results are consistent with the Born instability idea: melting is preceded by a continuous softening of the lattice with increasing temperature and volume. The crystal no longer has adequate rigidity to resist melting when one of its elastic shear moduli is sufficiently small albeit not zero.

Next, the relevance of the Lindemann melting criterion was examined by monitoring the T dependence of the Lindemann ratio δ_L, equal to the rmsd of a particle (at $\mathbf{r}_i$) from its equilibrium position (the ideal fcc lattice site $\mathbf{R}_i$), $\langle \Delta r^2\rangle^{1/2}$, divided by the averaged nearest-neighbor distance $\overline{r_{nn}} = 2^{-1/2}[4\Omega(T)]^{1/3}$. The result is shown in Fig. 2. At T_E, the system average δ_L is $\sim$0.12–0.13, consistent with the Lindemann criterion for equilibrium melting of simple crystals [2,11,12]. Upon superheating, δ_L continues to increase almost linearly with T up to $\delta_L \sim 0.2$, followed by a divergence upon melting. The value at T_m is about 0.22, almost 80% larger than the value at T_E but similar to the value for surface melting [2,23]. That is, to initiate melting without preexisting surfaces as heterogeneous nucleation sites, the bulk atoms have to rely on significant superheating to increase, through enhanced thermal vibrations, their rmsd to a level as high as that of surface atoms near T_E. Such a large rmsd appears to be a necessary condition which allows atoms to invade the spaces between their neighbors and therefore initiate melting.

The highly displaced particles near T_m can be further revealed by a non-Gaussian parameter of the form

$$\alpha_2(t) = \frac{3\langle \Delta r^4\rangle}{5\langle \Delta r^2\rangle^2} - 1, \qquad (2)$$

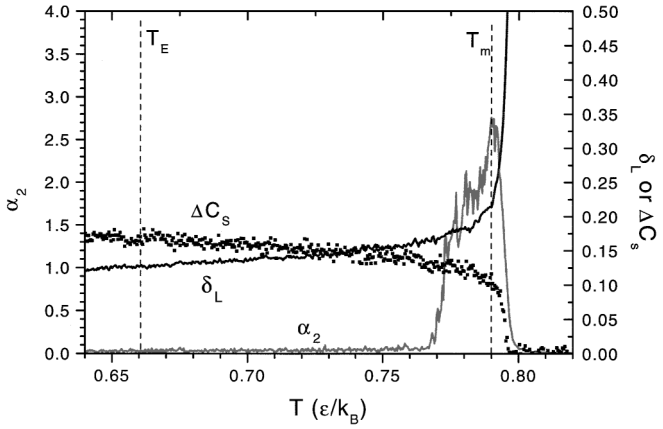

FIG. 2. The Lindemann parameter (δ_L), the effective shear modulus ΔC_S (squares), and α_2 versus temperature. See text.

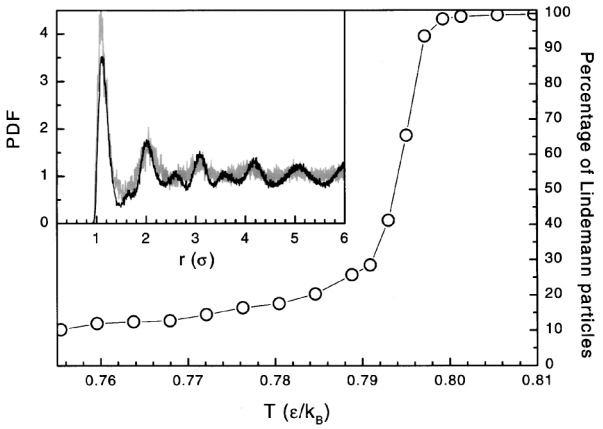

FIG. 3. Percentage of Lindemann particles as a function of temperature. Inset shows the PDFs for the Lindemann particles (gray line) and the non-Lindemann particles (black line), calculated for a snapshot at $T = 0.79$.

which is a simple correlation of the second and fourth moments of a 3D distribution of Δr $[= |\mathbf{r}_i(t) - \mathbf{R}_i|]$ with time t, which is zero for a Gaussian distribution. Large α_2 values are attributed to spatial or dynamical heterogeneities [24]. In our heating procedure T is a linear function of t and α_2 may therefore be calculated as a function of T. The α_2 result shown in Fig. 2 indicates a small value and a very weak T dependence below $T = 0.77$. A significant rise of α_2 occurred afterwards as the atomic movements became extensive with corresponding strong deviations from the equilibrium lattice sites. The broadened peak of α_2 over a T range of about 0.03 implies strong dynamical heterogeneities near the limit of superheating [24]. The α_2 continues to rise until melting, and then drops quickly to zero, indicating a complete loss of crystallinity in the random liquid. The δ_L corresponding to the α_2 peak defines the critical Lindemann ratio, $\delta_L^* = 0.22$.

Defining "Lindemann particle" as those with $\Delta r/\overline{r_{nn}} > \delta_L^*$, their population can be shown to increase with increasing T (Fig. 3). It is seen in the inset that the first peak of the pair distribution function (PDF) calculated among the Lindemann particles is higher than that among the non-Lindemann ones. This suggests a stronger spatial correlation of the Lindemann particles. Furthermore, the loss of peaks characterizing crystalline order in the PDF of the Lindemann particles indicates their more liquidlike location. While randomly emerging at low T, the Lindemann particles appear cooperatively and form extended clusters just before melting (where α_2 shows a peak). This scenario is displayed clearly in Fig. 4 which shows snapshots of the 3D atomic configurations taken at $T = 0.79$. The structural inhomogeneity suggests that melting does not occur all at once throughout a crystal but rather initiates via local instabilities. These Lindemann particles include, and are partly induced by, the interstitial point defects (at a lower population) discussed in analytical melting theories such as [25].

As already shown, the shear moduli difference ΔC_S goes to zero during melting. To see if this is satisfied preferentially by those Lindemann clusters, i.e., to further test the equivalence of the Born criterion and the Lindemann criterion, the Born moduli were calculated for each Lindemann particle. We observed that although the averaged ΔC_S (Fig. 2) for the system is far from zero at T_m, that for a cluster can be significantly lower and nearly zero if the cluster becomes sufficiently large (with more nearby Lindemann particles involved to move collectively, as indicated in Fig. 4).

These results demonstrate a strong correlation between the Lindemann criterion and the Born criterion: melting is initiated by local lattice instabilities governed by both. With increasing T, the number of Lindemann particles increases as the lattice continuously expands and softens. When the shear moduli become small enough (the Born instability), the destabilization of the particles becomes locally collective, promoting the formation of clusters which

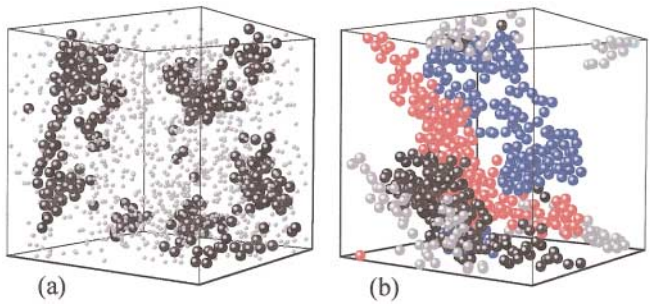

FIG. 4 (color). 3D visualization of the collective appearance of the Lindemann particles at $T = 0.79$. If the distance between a pair of the Lindemann particles is smaller than $(1 + \frac{1}{2}\delta_L^*)\overline{r}_{nn}$, they belong to the same cluster: (a) a few clusters with 20–200 particles (larger black circles) against other Lindemann particles (smaller gray circles) which do not form such clusters, and (b) four large clusters with 219, 214, 187, and 117 particles colored with red, blue, black and gray, respectively. Note that a cluster may appear in parts because of the periodic boundary conditions. The averaged ΔC_S for the whole system is 0.14; but the mean value for the clusters shown in (b) is only 0.05.

locally satisfy $C' = C_{44}$. In other words, the coinciding violation of both the vibrational and the shear elastic criteria sets the stage for the emergence of local regions that play the role of surfaces in initiating the equilibrium melting. The possible connection between these instability criteria has been proposed before [2,8,26], but our results constitute its first clear demonstration.

The observed intrinsic heterogeneous dynamics also provide an atomic-level perspective to view melting of a superheated solid as a process of homogeneous nucleation of the liquid phase [10]. The liquid embryos are formed microscopically by those thermally destabilized Lindemann particles, which appear in a cooperative way spatially, time wise, and energetically. Such a process has the effect of converting a second-order phase transition into a first-order one [27]. It was observed that at first such clusters are small, few and far between, and fluctuate in and out. As the superheating limit is approached, with the Born and Lindemann instabilities prevailing over larger and larger distances, the clusters expand, accumulate, and coalesce or percolate to eventually become the critical nuclei. A liquid nucleus consisting of about 300 particles at T_m is found to be stable to allow the growth of a liquid phase [28]. It is in reasonable agreement with the prediction of 200–500 particles by the classical homogenous nucleation theory at the maximum superheating [29].

To summarize, melting at the superheating limit is a first-order transition that results from clusters of destabilized particles, which are created thermally inside the bulk crystal due to simultaneous local vibrational and elastic lattice instabilities. At T_m, the clusters exhibit δ_L, ΔC_S, and elastic moduli similar to the surface atoms at T_E. They therefore have the same function as the surface atoms in the initiation of melting. The coalescence of a high density of such liquid embryos sets off massive homogeneous melt nucleation, which limits the maximum superheating observable.

Z. H. J. and K. L. thank the NSFC (598/599-31030), CAS, and the Max-Planck Society of Germany for support. E. M. is supported by the U.S. NSF (DMR-0080361).

*Email address: jin@finix.mpi-stuttgart.mpg.de

[1] For recent overviews, see, e.g., J. G. Dash, Rev. Mod. Phys. **71**, 1737 (1999).
[2] R. W. Cahn, Nature (London) **273**, 491 (1978); **323**, 668 (1986).
[3] J. Daeges *et al.,* Phys. Lett. A **119**, 79 (1986); L. Gråbæk *et al.,* Phys. Rev. B **45**, 2628 (1992).
[4] Z. H. Zhang and H. E. Elsayed-Ali, Surf. Sci. **405**, 271 (1998); L. Zhang *et al.,* Phys. Rev. Lett. **85**, 1484 (2000).
[5] C. W. Siders *et al.,* Science **286**, 1340 (1999); A. Rousse *et al.,* Nature (London) **410**, 65 (2001).
[6] J. L. Tallon, Nature (London) **342**, 658 (1989).
[7] H. J. Fecht and W. L. Johnson, Nature (London) **334**, 50 (1989).
[8] P. R. Okamoto *et al.,* Solid State Phys. **52**, 1 (1999); J. Wang *et al.,* Physica (Amsterdam) **240A**, 396 (1997).
[9] M. Born, J. Chem. Phys. **7**, 591 (1939); Proc. Cambridge Philos. Soc. **36**, 160 (1940).
[10] K. Lu and Y. Li, Phys. Rev. Lett. **80**, 4474 (1998); Z. H. Jin, K. Lu, Philos. Mag. Lett. **78**, 29 (1998).
[11] F. A. Lindemann, Z. Phys. **11**, 609 (1910); J. J. Gilvarry, Phys. Rev. **102**, 308 (1956); A. Voronel *et al.,* Phys. Rev. Lett. **60**, 3402 (1988).
[12] A. R. Abbelohda, *The Molten State of Matter: Melting and Crystal Structure* (Wiley, Chichester, 1978).
[13] D. Wolf *et al.,* J. Mater. Res. **5**, 286 (1990); J. Wang *et al.,* Phys. Rev. B **52**, 12 627 (1995).
[14] P. Stoltze, *Simulation Methods in Atomic Scale Materials Physics* (Polyteknisk Forlag, Lyngby, Denmark, 1997).
[15] To guarantee an overall smooth cutoff, a cutoff region, from $1.5r_0$ to $2.2r_0(2.47\sigma)$, was used following M. I. Baskes, Mater. Chem. Phys. **50**, 152 (1997); Phys. Rev. Lett. **83**, 2592 (1999). The equilibrium melting point was found to be $k_B T_E/\varepsilon = 0.66 \pm 0.02$, or $k_B T_E/E_0 \approx 0.0085$ (E_0 being the ground state cohesive energy) under the condition of coexisting solid and liquid phases, in good accordance with J. Q. Broughton and G. H. Gilmer, J. Chem. Phys. **79**, 5095 (1983); D. Chokappa and P. Clancy, Mol. Phys. **61**, 617 (1987).
[16] The time needed to melt the superheated crystal is about 1500τ, independent of heating rate. It corresponds to a melting rate of about 10^{13} m^3/s, or a melting front velocity of 2×10^4 m/s, for LJ argon. Despite the artificial effects from periodic boundary conditions, such a supersonic velocity agrees with experiments [5].
[17] M. Born and K. Huang, *Dynamical Theory of Crystal Lattices* (Clarendon, Oxford, 1954); J. Wang *et al.,* Phys. Rev. Lett. **71**, 4182 (1993).
[18] J. R. Ray, Comput. Phys. Rep. **8**, 109 (1988).
[19] M. S. Daw and M. I. Baskes, Phys. Rev. B **29**, 6443 (1984).
[20] T. Çağin and J. R. Ray, Phys. Rev. B **38**, 7940 (1988).
[21] In the LEM algorithm, whenever a particle has a negative component of the product vector of the momentum and the force, the corresponding velocity component is set to zero, e.g., [14].
[22] J. Q. Broughton and G. H. Gilmer, Model. Simul. Mater. Sci. Eng. **6**, 87 (1998).
[23] R. M. Goodman and R. M. Somorgai, J. Chem. Phys. **352**, 6325 (1970).
[24] A. Rahman, Phys. Rev. **136**, A405 (1964); W. Kob *et al.,* Phys. Rev. Lett. **79**, 2827 (1997). K. Zahn and G. Maret, Phys. Rev. Lett. **85**, 3656 (2000).
[25] A. V. Granato, Phys. Rev. Lett. **68**, 974 (1992); K. Nordlund and R. S. Averback, Phys. Rev. Lett. **80**, 4201 (1998).
[26] J. L. Tallon, Nature (London) **299**, 188 (1982); reply by R. M. J. Contterill and J. U. Madsen.
[27] See, e.g., F. R. N. Nabarro, *Theory of Crystal Dislocations* (Oxford University Press, London, 1967).
[28] This size, as well as T_m, was found independent of the system size (864, 2048, 6912, and 32 000 particles)
[29] At a superheating of $\Delta T = 0.2T_E$, the theory predicts a critical nucleus size of $n_c \sim 200$, assuming an interfacial energy σ_{ls} of 0.35 [J. Q. Broughton and G. H. Gilmer, Acta Metall. **31**, 845 (1983)], a latent heat per particle L of 1.0, and an atomic volume of $\Omega = 1.1$. With strain effects included [10], this number is $n_c \sim 500$.